Influence of post heat treatments on the microstructure and properties of Beta-Ti21S alloy produced by Laser Powder Bed Fusion for lightweight applications

Lorena Emanuelli[1], Alireza Jam[2], Vassili Tonon[2], Giorgio Valsecchi[3], Carlo Lora[4], Matteo Benedetti[2], Massimo Pellizzari[2]

[1] *INSTM (Operative center: University of Trento), Via Sommarive 9, 38123, Trento (TN), Italy*
[2] *University of Trento, Via Sommarive 9, 38123, Trento (TN), Italy*
[3] *TAV, Via dell'industria 11, 24043, Caravaggio (BG), Italy*
[4] *SISMA S.p.A., Via dell'industria 1, 36013, Piovene Rocchette (VI), Italy*

Beta Ti alloys are of great interest for many applications where high temperature strength, creep resistance, thermal stability and oxidation resistance are required. Recently, we demonstrated the good 3D printability of Ti21S alloy (Ti-15Mo-3Nb-3Al-0.2Si (wt.%)) by Laser Powder Bed Fusion (L-PBF), Nevertheless, the rapid heating and solidification rate achieved during the L-PBF process promote the microstructural and structural anisotropy, microsegregation and residual stress formation deleterious for the performances of the components. In addition, as-built Ti-21S alloy is characterized by an unwanted strain softening behavior after yielding. The application of a post heat treatment becomes fundamental to optimize the microstructure and improve the mechanical properties.

In this study, the influence of different heat treatments on the microstructure and mechanical properties of metastable β Ti-21S alloy fabricated by laser powder bed fusion (L-PBF) was investigated. Solution heat treatment temperatures and aging temperatures were modified to define the most promising heat treatment for orthopedic implant. Direct Artificial Aging (AA) was selected as the most promising heat treatment thanks to the high yield strength of about 1200 MPa without loss of ductility. Based on this, the effect of AA on the mechanical response of a cellular structure was investigated. The AA leads to a considerable improvement of the compression-compression fatigue strength.

Keywords: *metastable beta titanium alloys, Ti-21S, heat treatments, lightweight application, cellular structure, laser powder bed fusion*

1. Introduction

Beta titanium alloys are widely used in biomedical, aerospace, marine and automotive industries thanks to their high specific strength, extraordinary toughness and good corrosion resistance [1]. Among these β-alloys, the metastable β Ti-21S, characterized by a chemical composition of Ti-15Mo-3Nb-3Al-0.2Si (wt.%), has growing interest in a variety of applications thanks to its high temperature strength, creep resistance, thermal stability, oxidation resistance, low stiffness and good biocompatibility [2,3]. In the industries where beta titanium alloys are usually used, due to the necessity to produce very complex geometries, additive manufacturing technologies are becoming the main production processes. For instance, Laser Powder Bed Fusion (L-PBF) permits to produce components with optimized geometry to increase the strength to weight ratio by producing cellular or porous structure inside the component and excellent dimensional precision and accuracy [4]. Nevertheless, the rapid heating and solidification rate occurring during the L-PBF technology leads to a microstructural and structural anisotropy, microsegregation and residual stresses that result deleterious for the performances of the components [5]. Additively manufactured (AMed) Ti-21S alloy was studied by Pellizzari et. al. [3] showing a low elastic modulus e good mechanical properties interesting for biomedical applications. Nevertheless, strengthening of this alloy by precipitation hardening could be achieved through specific heat treatments. A lot of investigations were conducted on the effect of different heat treatments on cast and wrought Ti-21S alloy [6,7]. Solution heat treatment (SHT) above the β-transus followed by artificial aging (AA) between 500 and 700°C is the common heat treatment suggested. SHT has the aim to recrystallize and homogenize the microstructure and the ageing is focused on the strengthening of the material through the precipitation of well distributed α phase inside grains. Not only α phase precipitation occurs during heat treatment but also the formation of ω phase takes place in a specific temperature range. The precipitation and consequently dissolution of ω phase acts as a heterogeneous nucleation for a finer α phase. Nevertheless, a drastic decrease of the ductility occurs if ω phase is not completely replaced by α phase [8]. Very few authors studied the effect of different heat treatments on the microstructure and mechanical properties of AMed Ti-21S alloy [9]. For this reason, in this work, the influence of different heat treatments on the microstructure and mechanical properties of metastable β Ti-21S alloy fabricated by laser powder bed fusion (L-PBF) was investigated. Different aging temperatures and effect of solution heat treatment (SHT) before ageing were studied and the positive effect of the most promising heat treatment on the fatigue resistance of a cellular structure, namely octet truss, design for biomedical application was investigated.

2. Material and Method

A β-Ti21S pre-alloyed powder (GKN Hoeganaes Corporation, USA, D_{10}=25 µm, D_{50}=41 µm, D_{90}=60 µm) was used. Dog-bone (ASTM E8M) samples and octet truss cellular samples were 3D printed with the main axis parallel to the building direction (BD) using a L-PBF machine model SISMA MYSINT100 on a platform of 100 mm in Ar atmosphere. A laser spot of 55 µm, a power of 200W, a volume energy density between 40 and 90 J/mm^3 and a 90° scanning strategy were used. Heat treatments were carried out in a TAV vacuum furnace equipped with an all-metal molybdenum hot zone. Effect of ageing temperatures on the mechanical properties and microstructure was evaluated by performing three different heat treatments with aging temperature of 350°C, 420°C and 650°C for 2h (HT1, HT2, HT3). After the individuation of the most promising ageing temperature, two industrial heat treatments were performed with and without a solution heat treatment (SHT) before direct artificial ageing, named STA and AA, respectively. Details of all heat treatments are summarized in Table 1.

Table 1 Heat treatments of tensile specimens. if not specified, heating rate is equal to 10°C/min and cooling rate of 30 °C/min

HTs	SHT	AA
HT1	-	350°C x 2h
HT2		420°C x 2h
HT3	-	650°C x 2h
STA	930°C x 30 min RT in 6 min	590°C x 8h
AA	-	590°C x 8h

* RT room temperature (RT); ** FC Furnace cooling.

Tensile tests were carried out according to ASTM E8 at RT, with a strain rate of 1 mm/min and using an extensometer with a 12.5 mm gauge length to evaluate the elastic region of the curves. After sandblasting, one sample for HT1, HT2 and HT3 and three samples for as built (AB), STA and AA were tested. The microstructural characterization was carried out by scanning electron microscopy (SEM) after proper metallographic preparation. High cycle compression-compression fatigue testing on octet truss cellular structure was performed using a Rumul Testronic resonant fatigue test machine equipped with a 50 kN load cell with an R-ratio of 0.1 in compression. Fatigue tests were run in laboratory environment at various stress amplitudes to evaluate fatigue lives ranging from 10^5 to 10^7 cycles.

3. Results and Discussion

Tensile nominal stress-strain curves of the AB and HTs samples are reported in Figure 1.

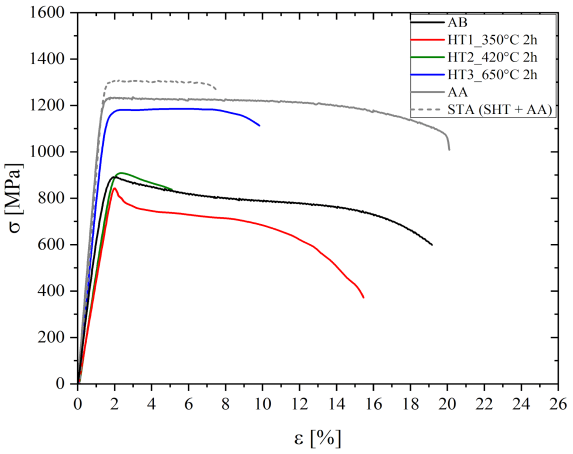

Figure 1 nominal stress-strain curve of AB and HTs samples.

The corresponding mechanical properties are summarized in Table 2.

Table 2 Mechanical properties of β-Ti21S obtained by L-PBF in AB condition and after different HTs.

	E(GPa)	σy[MPa]	UTS[MPa]	ε_R [%]
AB	64 ± 1	804 ± 29	894 ± 13	21.6 ± 0.8
HT1	62	815	840	15.5
HT2	62	850	907	5.0
HT3	97	1120	1180	9.8
STA	96 ± 0	1286 ± 6	1301 ± 7	6.7 ± 0.8
AA	96 ± 1	1208 ± 19	1235 ± 15	21.0 ± 1.2

Considering the AB material (black curve), after the elastic region shows a very intense work softening highlighted by a marked stress drop. As reported in literature, this is ascribed to the planar inhomogeneous plastic flow enhanced by an increased localized adiabatic temperature [10]. Comparing the AB curve with those of HT1 (red curve), HT2 (green curve) and HT3 (blue curve) it is evident that only after ageing at 650°C (HT3) is possible to remove the softening behavior, achieving increased strength and limited drop in the ductility. The high drop of ductility observed after ageing temperature at 420°C (HT2) can be ascribed to the precipitation of ω phase in the range of 200-400°C. As demonstrated in a previous work, a higher ageing temperature, comprised between 500 and 650°C allows the dissolution of this phase that act as heterogeneous nucleation site for the precipitation of α, confirmed by the higher Young modulus (Tabel 2) [9]. The artificial ageing in STA and AA is carried out at 590 °C, where α precipitation takes place [9]. The comparison between STA and AA highlights a higher strength followed by a marked drop in ductility in case of STA. This behavior could be justified considering the microstructure achieved after STA and AA (Figure 2).

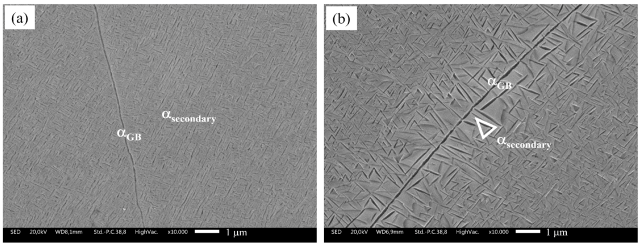

Figure 2 SEM micrographs of a) AA and b) STA samples

SEM micrograph of AA sample (Figure 2a) highlights presence of banded and Widmanstätten α phase with a size lower than 1 µm inside β grains confirming a predominant intragranular precipitation along specific directions with some presence of thin and discontinuous α_{GB}. Differently, formation of a secondary α with the peculiar triangular α lamellae arrangements and a thicker and continuous film of α_{GB} are observed in STA sample (Figure 2b). The continuous α_{GB} film obtained due to a poor quench after SHT is responsible for the high drop of ductility observed in Figure 1 (gray dotted curve) and the triangular secondary α justified the higher strength respect to the AA. Based on this, AA results in the most promising heat treatment to increase the strength of the AMed Ti-21S alloy without loss in ductility.

The positive effect of AA was evaluated also on the fatigue resistance of a octet truss cellular structure (Figure 3a) designed for lightweight applications. The results of compression-compression high cycle fatigue tests normalized with respect to the compression yield strength for the octet truss cellular structure before and after AA are plotted in Figure 3b.

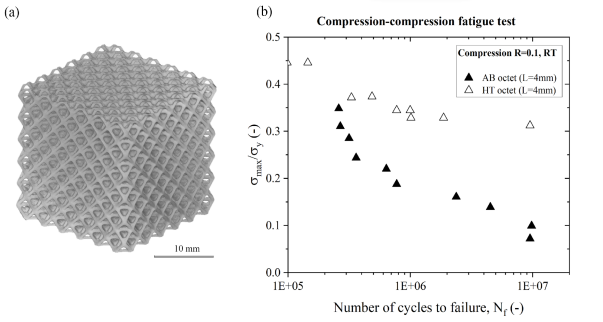

Figure 3 a) Micro-CT of octet truss sample, b) compression-compression high cycles fatigue resistance of AB and AA octet truss samples.

It is evident that the AA considerably improves the fatigue resistance. The normalization with respect to the yield strength highlights that the improvement of the fatigue strength is due to the suppression of the strain softening occurring during AA. Indeed, in the AB sample, the expansion of the localized plasticization occurring at the nodes of the structure due to the high stress concentration expands at each fatigue cycle due to the strain softening effect.

4. Conclusions

In this study, the influence of post heat treatments on the mechanical properties and microstructure of a β-Ti21S fabricated by L-PBF was investigated. The best post heat treatment results the Direct Artificial Ageing (AA). To achieve the desired results, the ageing temperature needed to be higher than 500°C. This higher temperature is necessary to dissolve the brittle ω phase and to promote the heterogeneous nucleation of a well-distributed α phase within the β grains. Another advantage of the AA treatment is that it can prevent strain softening, a phenomenon that occurs in the AB condition. Strain softening can lead to reduced strength and increased plastic deformation, making the material more susceptible to fatigue failure. By using AA, strain softening can be suppressed, and this positively affects the fatigue strength of octet truss cellular structures. Moreover, the treatment reduces localized plasticization in the nodes of the cellular structures, further improving their mechanical performance.

Acknowledgments

This work is part of the project N. 2020.0042 - ID 50430, “Produzione additiva di protesi ortopediche a struttura trabecolare in Ti-beta” funded by Fondazione Cariverona.

References

[1] F.H. Sam Froes, M. Qian, M. Niinomi, Titanium for consumer applications: Real world use of titanium, Titan. Consum. Appl. Real-World Use Titan. (2019) 1–349.

[2] M.A. Macias-Sifuentes, C. Xu, O. Sanchez-Mata, S.Y. Kwon, S.E. Atabay, J.A. Muñiz-Lerma, M. Brochu, Microstructure and mechanical properties of β-21S Ti alloy fabricated through laser powder bed fusion, Prog. Addit. Manuf. 6 (2021) 417–430.

[3] M. Pellizzari, A. Jam, M. Tschon, M. Fini, C. Lora, M. Benedetti, A 3D-printed ultra-low young’s modulus β-Ti alloy for biomedical applications, Materials (Basel). 13 (2020) 1–16.

[4] J. V. Gordon, S.P. Narra, R.W. Cunningham, H. Liu, H. Chen, R.M. Suter, J.L. Beuth, A.D. Rollett, Defect structure process maps for laser powder bed fusion additive manufacturing, Addit. Manuf. 36 (2020).

[5] J. Pelleg, Additive and Traditionally Manufactured Components: A Comparative Analysis of Mechanical Properties, Addit. Tradit. Manuf. Components A Comp. Anal. Mech. Prop. (2020) 1–642.

[6] T.W. Xu, H.C. Kou, J.S. Li, F.S. Zhang, Y. Feng, Effect of Phase Transformation Conditions on the Microstructure and Tensile Properties of Ti-3Al-15Mo-3Nb-0.2Si Alloy, J. Mater. Eng. Perform. 24 (2015) 3018–3025.

[7] T. Xu, S. Zhang, S. Liang, N. Cui, L. Cao, Y. Wan, Precipitation behaviour during the β → α/ω phase transformation and its effect on the mechanical performance of a Ti-15Mo-2.7Nb-3Al-0.2Si alloy,

Sci. Rep. 9 (2019) 1–12.
[8] R. Dong, J. Li, H. Kou, J. Fan, Y. Zhao, H. Hou, L. Wu, ω-Assisted refinement of α phase and its effect on the tensile properties of a near β titanium alloy, J. Mater. Sci. Technol. 44 (2020) 24–30.
[9] M. Pellizzari, A. Jam, V. Tonon, M. Benedetti, C. Lora, Ageing behavior of Beta-Ti21S produced by laser powder bed fusion, Metall. Ital. (2021).
[10] S.S.S. Kumar, B. Pavithra, V. Singh, P. Ghosal, T. Raghu, Tensile anisotropy associated microstructural and microtextural evolution in a metastable beta titanium alloy, Mater. Sci. Eng. A. 747 (2019) 1–16.